

## Negative thermal quenching of below-bandgap photoluminescence in InPBi

Xiren Chen,<sup>1,2</sup> Xiaoyan Wu,<sup>2</sup> Li Yue,<sup>2</sup> Liangqing Zhu,<sup>1,3</sup> Wenwu Pan,<sup>2</sup> Zhen Qi,<sup>1</sup> Shumin Wang,<sup>2,4,a)</sup> and Jun Shao<sup>1,b)</sup>

<sup>1</sup>National Laboratory for Infrared Physics, Shanghai Institute of Technical Physics, Chinese Academy of Sciences, 200083 Shanghai, China

<sup>2</sup>State Key Laboratory of Functional Materials for Informatics, Shanghai Institute of Microsystem and Information Technology, Chinese Academy of Sciences, 200050 Shanghai, China

<sup>3</sup>Key Laboratory of Polar Materials and Devices, East China Normal University, 200062 Shanghai, China

<sup>4</sup>Photonic Laboratory, Department of Microtechnology and Nanoscience, Chalmers University of Technology, S-412 96 Göteborg, Sweden

(Received 3 November 2016; accepted 23 January 2017; published online 1 February 2017)

This paper reports a temperature-dependent (10–280 K) photoluminescence (PL) study of below-bandgap electron-hole recombinations and anomalous negative thermal quenching of PL intensity in  $\text{InP}_{1-x}\text{Bi}_x$  ( $x = 0.019$  and  $0.023$ ). Four PL features are well resolved by curve-fitting of the PL spectra, of which the energies exhibit different temperature dependence. The integral intensities of the two high-energy features diminish monotonically as temperature rises up, while those of the two low-energy features decrease below but increase anomalously above 180 K. A phenomenological model is established that the residual electrons in the final state of the PL transition transfer into nonradiative state via thermal hopping, and the thermal hopping produces in parallel holes in the final state and hence enhances the radiative recombination significantly. A reasonable interpretation of the PL processes in InPBi is achieved, and the activation energies of the PL quenching and thermal hopping are deduced. *Published by AIP Publishing.* [<http://dx.doi.org/10.1063/1.4975586>]

Temperature-dependent photoluminescence (PL) as a powerful probe has been widely employed for characterizing electron-hole recombinations in semiconductors. In particular, the evolution of PL intensity with temperature reveals nonradiative recombination mechanisms:<sup>1–3</sup> as temperature rises up, the nonradiative centers in semiconductor capture carriers result in a monotonic quenching to the PL integral intensity. The quenching can be described by a multi-center model<sup>4,5</sup>

$$I(T) = I_0 / (1 + C_q e^{-E_q/k_B T}), \quad (1)$$

where  $I_0$  is the integral intensity before quenching,  $C_q$  is the nonradiative coefficient being relevant to the carriers lifetime, capture coefficient and effective density of states, and  $k_B$  and  $E_q$  are Boltzmann constant and activation energy of the quenching, respectively.

Dilute-bismuth (Bi) III–V semiconductors are very promising for possible long-wavelength opto-electronic applications of laser diode,<sup>6</sup> light emitting diode,<sup>7</sup> and photodetector,<sup>8</sup> due to the Bi-induced bandgap shrinkage and spin-orbit enhancement.<sup>9–11</sup> The PL evolution with temperature in dilute-Bi III–V semiconductors has attracted extensive attention.<sup>12–14</sup> For example, it was clarified for GaAsBi that the thermal quenching of bandedge PL is due to two-energy components of cluster localization and alloy disorder.<sup>12</sup> For  $\text{InP}_{1-x}\text{Bi}_x$ , which is compatible with InP-based devices and the bandgap reduction is as large as 60–80 meV/%Bi,<sup>15–19</sup> however, the bandedge PL emission is missing and an extraordinarily broad below-bandgap PL emission shows up

in a range of 0.9–2.5  $\mu\text{m}$ .<sup>15–17</sup> While such a broad-band PL emission may open up a new application window for, e.g., super-broad infrared source covering the whole telecommunication spectral range, the thermal quenching of the broad-band PL is yet to be clarified.

We in this paper report a temperature-dependent PL study of two  $\text{InP}_{1-x}\text{Bi}_x$  ( $x = 0.019$  and  $0.023$ ) epilayers, with a focus on the integral intensity evolution of the below-bandgap PL transitions. The PL integral intensity diminishes with temperature monotonically in the range below about 180 K but gets enhanced anomalously as temperature goes beyond 180 K. A phenomenological model is established based on the thermal hopping of residual electrons and is verified by the excitation-dependent PL experiment, by which the mechanism of the PL evolution is clarified.

Two  $\text{InP}_{1-x}\text{Bi}_x$  ( $x = 0.019$  and  $0.023$ ) epilayers were grown for this study on InP:Fe substrates by molecular beam epitaxy. To implement effective Bi incorporation, the growth temperature was set at 275 °C, which is much lower than the optimized growth temperature for InP.<sup>15</sup> The epitaxial thickness is about 200 nm, and the Bi content  $x$  is deduced by high-resolution X-ray diffraction. For temperature-dependent PL measurements, the samples were, together with a small piece of InP:Fe substrate as reference, mounted in a continuous-flow liquid-helium dewar, and a Fourier transform infrared spectrometer-based PL system was employed running in the continuous-scan mode.<sup>20,21</sup> A  $\text{Kr}^+$  laser together with a laser-power controller was selected to warrant a stable excitation. An optical band-pass filter was used for rejecting environmental thermal emission, and an InSb detector was configured for PL signal detection.

Figure 1 shows the PL spectra of the two  $\text{InP}_{1-x}\text{Bi}_x$  ( $x = 0.019$  and  $0.023$ ) samples at 10 K under a nominal

<sup>a)</sup>Electronic mail: shumin@mail.sim.ac.cn

<sup>b)</sup>Author to whom correspondence should be addressed. Electronic mail: jshao@mail.sitp.ac.cn

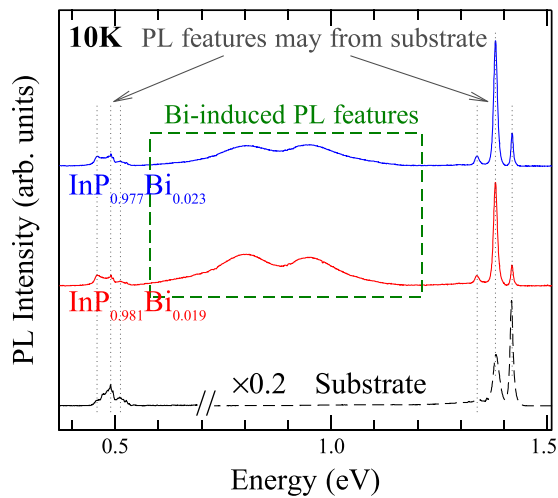


FIG. 1. PL spectra of  $\text{InP}_{1-x}\text{Bi}_x$  ( $x = 0.019$  and  $0.023$ ) samples and  $\text{InP:Fe}$  substrate at 10 K. The peaks at 1.419, 1.380, and 1.338 eV, and the features around 0.5 eV as well, are substrate related. The dashed box emphasizes Bi-induced PL features in  $\text{InPBi}$ . The dashed part of the substrate PL is magnified by 0.2 for similar height around 1.4 eV.

excitation of 100 mW. For comparison, a PL spectrum from the  $\text{InP:Fe}$  substrate is depicted and the part around the band gap of  $\text{InP}$  is magnified by 0.2 for a similar peak height at about 1.4 eV as those of the  $\text{InPBi}$  samples.

With the aid of the substrate PL spectrum, it is clear that neither the three PL peaks at 1.419, 1.380, and 1.338 eV nor the PL features around 0.5 eV of the  $\text{InPBi}$  samples are the direct effects of Bi incorporation in  $\text{InP}$ . The PL peaks coincide energetically with those of the  $\text{InP:Fe}$  substrate and may be due to band-to-band and band-to-shallow level transitions in  $\text{InP}$ . The PL features at about 0.5 eV also show up in the substrate PL and may be correlated with the Fe-related transitions in  $\text{InP:Fe}$ .<sup>22</sup>

The broad bimodal PL features as enclosed by the dashed rectangle in Fig. 1 are only seen in the  $\text{InPBi}$  samples and were not seen in the previous studies of  $\text{InP}$  films grown at similar low temperatures.<sup>15,16</sup> Consequently, it hints a direct correlation of the bimodal-PL features with Bi doping. As the energies of the two humps are about 0.80 and 0.96 eV, respectively, which are far below the expected  $\text{InP}_{1-x}\text{Bi}_x$  ( $x = 0.019$  and  $0.023$ ) bandgap,<sup>18,19</sup> the bimodal-PL features should accordingly be relevant to Bi-induced defects rather than the bandgap shrinkage.<sup>11</sup>

To have a closer view of the Bi-induced below-bandgap PL transitions, temperature-dependent PL measurements are conducted and the PL spectra are depicted in Fig. 2 for the  $\text{InP}_{0.981}\text{Bi}_{0.019}$  (a) and  $\text{InP}_{0.977}\text{Bi}_{0.023}$  (b) samples, respectively.

As temperature rises up in the range of 10–180 K, the PL features diminish monotonically, of which the high-energy hump manifests a faster quenching and disappears at high temperatures. In the temperature range above 180 K, however, a bulge at about 0.64 eV shows up, conjoins with the low-energy hump, and gets enhanced steadily with temperature. Such an anomalous intensity enhancement was previously denoted as negative thermal quenching<sup>23</sup> and can be analyzed quantitatively by curve-fitting treatments of the PL spectra with an assumption of Gaussian-Lorentzian lineshape

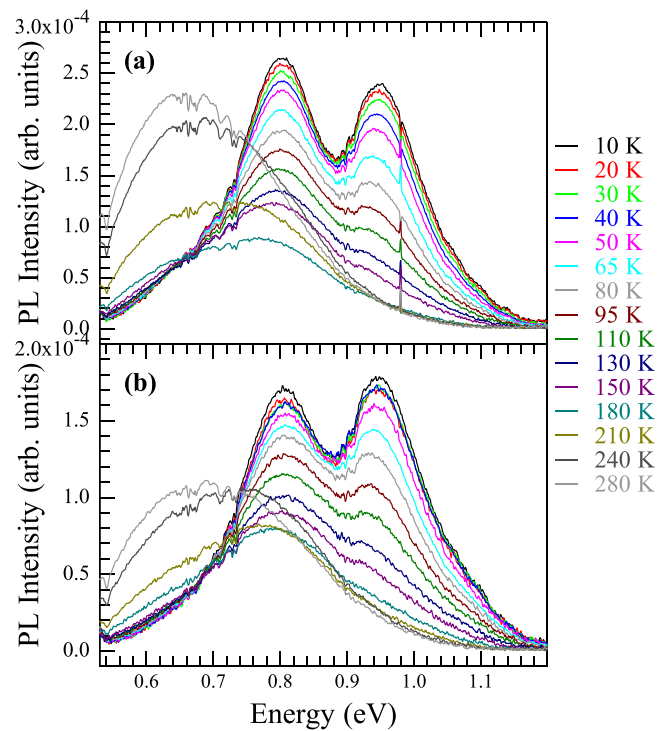


FIG. 2. Temperature-dependent below-bandgap bimodal PL features of  $\text{InP}_{0.981}\text{Bi}_{0.019}$  (a) and  $\text{InP}_{0.977}\text{Bi}_{0.023}$  (b). The wrinkles around 0.7 eV are caused by atmospheric disturbance.

to each individual PL feature.<sup>21,24</sup> The Gaussian-Lorentzian lineshape is given by<sup>25</sup>

$$f(E) \propto s \cdot e^{-\ln 2 \left( \frac{E-E_0}{w_h} \right)^2} + \frac{1-s}{1 + \left( \frac{E-E_0}{w_h} \right)^2}, \quad (2)$$

where the first and second terms on the right side represent the Gaussian and Lorentzian contents and reflect the inhomogeneous and homogeneous broadening effects, respectively.<sup>26</sup>  $E_0$  is the PL peak energy,  $w_h$  is the half-width at half-maximum and  $0 \leq s \leq 1$  is the Gaussian shape factor.

Figure 3(a) shows representative curve fittings of the Bi-induced below-bandgap PL features for the  $\text{InP}_{0.981}\text{Bi}_{0.019}$  sample. Curve fittings for the other sample lead to similar results. At 10 K, four broad PL features peaking at 0.707, 0.806, 0.949, and 1.045 eV, respectively, are necessary for a good fit and are labeled as A-, B-, C-, and D-feature for clarity. As temperature rises up, the A-feature first diminishes slightly but exhibits significant negative thermal quenching when the temperature gets higher than 130 K. The B-feature shows negative thermal quenching only in the temperature range well above 180 K with less significance. The C- and D-features, on the other hand, diminish monotonically, and the D-feature even disappears as the temperatures gets beyond 130 K.

The energy of each fitting PL feature is plotted against temperature in Fig. 3(b), which shows approximately linear redshift with temperature, and the slope is marked correspondingly. It is worthy to emphasize that such redshifts are very weak with respect to that of the band gap and may hint that the PL features are related to the impurities levels in  $\text{InPBi}$ .<sup>27,28</sup> With the matters of facts in mind that (i) the four

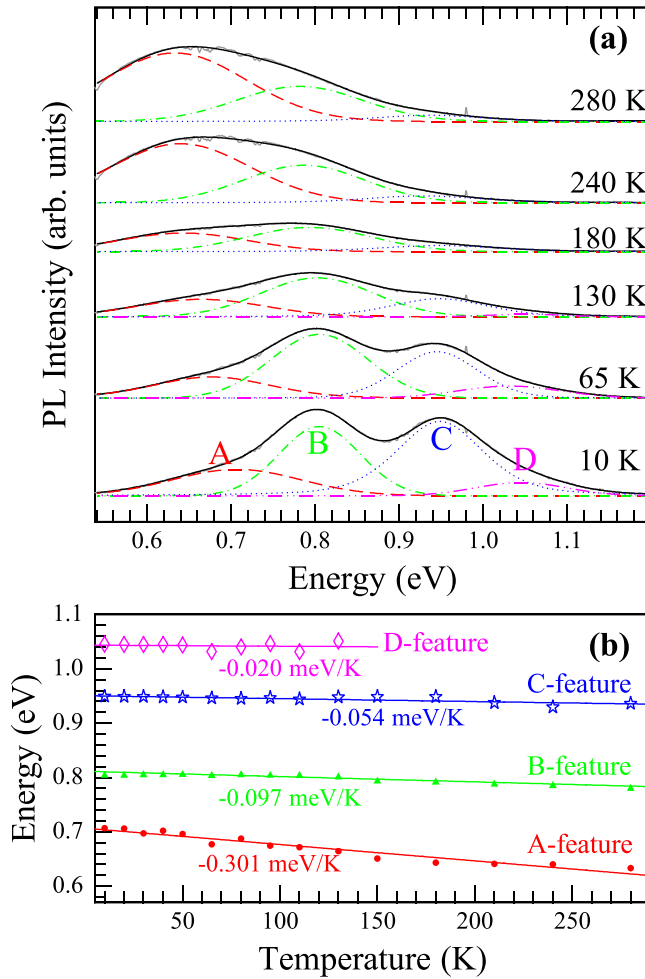


FIG. 3. (a) Curve-fittings of PL spectra for InP<sub>0.981</sub>Bi<sub>0.019</sub> at representative temperatures, with an assumption of Gaussian-Lorentzian lineshapes. A- and B-features show significant negative thermal quenching, while C- and D-features diminish monotonically as temperature rises up. (b) Energy vs. temperature of the fitting PL features, solid lines for linear fits with the slopes being marked. The slopes hint that the PL features are related to the impurities levels.

below-bandgap PL features are Bi-induced, (ii) V<sub>III</sub> anti-site is expected to be a donor in dilute-Bi semiconductors grown at low temperatures,<sup>29</sup> and (iii) Bi pairs/clusters as common defects lead to acceptor levels above the valence band,<sup>30</sup> we conclude that the final states of the below-bandgap PL transitions are relevant to the acceptor levels, while the initial states correlate with the donor levels inherent in low-temperature grown InPBi and draw as below a phenomenological model for the negative thermal quenching in InPBi.

Low-temperature growth introduces unavoidably high-density donor-type impurities<sup>31</sup> and leads to the n-type characteristics of InPBi.<sup>32</sup> The Fermi level is hence close to the conduction band, and the Bi pairs/clusters-induced acceptor levels are filled by electrons in the steady state. During the PL process, the electrons in the valence band are first pumped by laser irradiation into the conduction band and then relaxed into the initial states. Meanwhile, the electrons in the acceptor levels relax nonradiatively to the pumping-induced holes in the valence band, as schematically shown in Fig. 4(a). Although the density of Bi pairs/clusters in InPBi is not known quantitatively, it should be obviously higher than that of the pumping-induced electrons generally at a

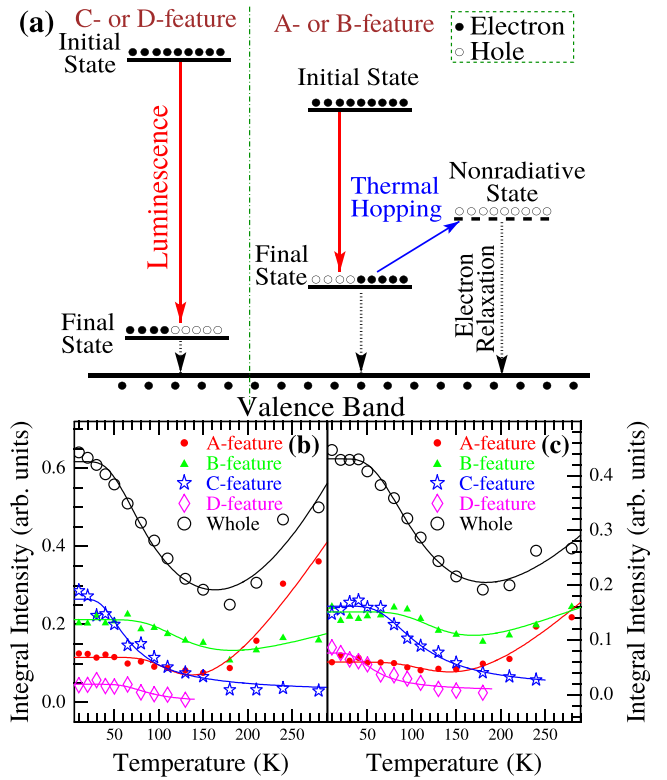


FIG. 4. (a) Schematic PL thermal quenching in InPBi, with red, blue, and dashed arrows for the PL of initial-final state, the electrons thermally hopping from final to nonradiative state, and nonradiative relaxation of electrons, respectively. (b) and (c) Evolution of integral intensities with temperature and theoretical fits (lines) for the PL features and the whole PL in InP<sub>1-x</sub>Bi<sub>x</sub> ( $x = 0.019$  and  $0.023$ ). Results indicate that Eq. (4) reproduces the temperature-dependent PL integral intensity quite well.

level of  $\sim 10^{16} \text{ cm}^{-3}$  because (i) no band-to-band PL transition is detected and (ii) the Bi pairs/clusters density was reported to be  $\sim 10^{18} \text{ cm}^{-3}$  in a similar material of GaAsBi.<sup>30</sup> In consequence, there should be massive residual electrons in the acceptor levels acting as the final states for the below-bandgap PL transitions.

The C- and D-features of InPBi are due to the recombinations of the electrons in the initial states with the holes in the final states. The PL integral intensity quenches monotonically and can be well described by Eq. (1) with one nonradiative channel. For the A- and B-features, an interaction between the (radiative) final state and the nonradiative state in InPBi has to be considered. At low temperatures, the residual electrons in the final state do seldom transfer to the nonradiative state, and hence the PL originates in the recombination of the initial-state electrons with the final-state holes, and due to the nonradiative recombination, the integral intensity diminishes monotonically as temperature rises up. At high temperatures, however, the thermal hopping is activated and the residual electrons in the final state transfer to the nonradiative state, as schematically shown by the blue-arrow in Fig. 4(a). This leads to additional holes in the final state and therefore an enhancement to the corresponding PL transition. The PL recombination rate ( $R$ ) and hence the integral intensity of initial-to-final state ( $I$ ) can be described as  $I \propto R \propto n^{\text{IS}} p^{\text{FS}}$ , where  $n^{\text{IS}}$  and  $p^{\text{FS}}$  are the densities of electron in the initial and hole in the final states, respectively. The thermal hopping of the residual electrons from the final

state produces additional holes, and as a result the density of holes increases in the final state. Based on the Shibata's model,<sup>23</sup> the electrons thermally hopping to nonradiative state can be described with  $n_{re}^{FS} e^{-E_h/k_B T}$ , where  $n_{re}^{FS}$  stands for the density of residual electrons in the final state and  $E_h$  the activation energy of thermal hopping. The density of holes in the final state is therefore given by

$$p^{FS} = p_0^{FS} + n_{re}^{FS} e^{-E_h/k_B T}, \quad (3)$$

where  $p_0^{FS}$  is the initial density without thermal hopping.

It is now obvious that with the thermal hopping, Eq. (1) can be rewritten as<sup>23</sup>

$$I(T) = I_0 \frac{1 + C_h e^{-E_h/k_B T}}{1 + C_q e^{-E_q/k_B T}}, \quad (4)$$

where  $C_h$  is a hopping coefficient being relevant to the density of residual electrons and decreases steadily due to the depletion of the residual electrons in the final state, as the temperature rises up. Correspondingly, the PL intensity should quench at high enough temperatures. This is in fact the case for the C- and D-features, for which the thermal hopping is negligible. For the A- and B-features, on the other hand, the PL intensity gets even enhanced around room-temperature (RT). This indicates that the depletion of the residual electrons is not significant in the final state, and  $C_h$  can be assumed as a constant for simplicity in the temperature range being considered.

Figures 4(b) and 4(c) depict the fittings to the PL-feature integral intensities by Eq. (4). Obviously, the model reproduces quite well both the monotonic quenching of the C- and D-features and the non-monotonic evolution of the A- and B-features as well as the whole PL of two  $\text{InP}_{1-x}\text{Bi}_x$  samples, with the fitting parameters, as listed in Table I. This provides a direct support to the thermal hopping model.

To further verify the rationality of the phenomenological model, excitation power-dependent PL measurements are conducted at 10 K and RT, respectively. According to the model, the density of holes in the valence band should be low, and hence an enhancement of the residual electrons occurs in the final state at low excitation. Consequently, the thermal hopping is reinforced and more significant negative thermal quenching effect shows up. This is indeed the real observation in the excitation power-dependent PL spectra, as illustrated in Fig. 5 for the  $\text{InP}_{0.981}\text{Bi}_{0.019}$  sample under excitation power of 30 and 120 mW: at the low excitation of 30 mW, the PL intensity at RT is close to that at 10 K, while at

TABLE I. Fitting parameters for the intensities of PL features and the whole PL in  $\text{InP}_{1-x}\text{Bi}_x$  ( $x=0.019$  and  $0.023$ ).  $C_h$  and  $C_q$  are dimensionless constants, and  $E_h$  and  $E_q$  are in meV.

$x$	0.019/0.023				
	A	B	C	D	Whole
$C_h$	5817/954	82/127	...	...	81/45
$E_h$	113/102	80/82	...	...	90/85
$C_q$	173/32	28/36	11/21	85/16	6/7
$E_q$	58/46	47/52	16/31	35/17	19/25

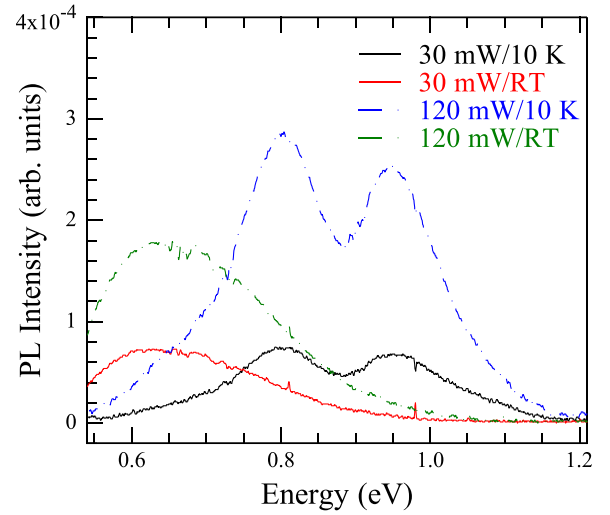


FIG. 5. PL spectra of  $\text{InP}_{0.981}\text{Bi}_{0.019}$  at 10 K and RT with nominal excitation of 30 and 120 mW, respectively. More significant negative thermal quenching is seen at low excitation, in agreement with the above-established model.

120 mW the PL intensity at RT is only about 65% of that at 10 K.

A brief conjecture about the initial and final states can be made for the below-bandgap PL features of InPBi. The deduced bandgap of  $\text{InP}_{0.981}\text{Bi}_{0.019}$  is about 1.25 eV.<sup>16,18</sup> The native  $\text{P}_{\text{In}}$  donor level was indicated to be about 0.2–0.3 eV below the conduction band,<sup>17,31</sup> and the acceptor level due to Bi pairs/clusters was found at about 0.11 eV above the valence band in  $\text{InP}_{0.975}\text{Bi}_{0.025}$ .<sup>17</sup> In addition, theoretical simulations suggested that the  $\text{Bi}_{\text{In}}$  anti-site exists in InPBi and the energetic level is located at about 0.39 eV below the conduction band of InPBi at RT.<sup>33</sup> It therefore seems to be a hint that the A- and B-features may be attributed to the  $\text{Bi}_{\text{In}}$ -to-Bi pairs/clusters and  $\text{P}_{\text{In}}$ -to-Bi pairs/clusters transitions, respectively; and C- and D-features the  $\text{Bi}_{\text{In}}$ - and  $\text{P}_{\text{In}}$ -levels to the Bi pairs/clusters-irrelevant shallow-acceptor levels transitions. The negative thermal quenching of the A- and B-features implies that the Bi pairs/clusters produce not only acceptor levels but also significant nonradiative states in InPBi. The sample-dependent  $E_h$  and/or  $E_q$  of the corresponding PL features may reflect the Bi effect on the radiative recombination, and the less significant negative thermal quenching in  $\text{InP}_{0.977}\text{Bi}_{0.023}$  may be due to the surfactant effect of Bi that reduces the density of nonradiative state and hence the hopping possibility.<sup>15</sup>

To summarize, temperature-dependent (10–280 K) PL analysis of the below-bandgap transitions in  $\text{InP}_{0.981}\text{Bi}_{0.019}$  and  $\text{InP}_{0.977}\text{Bi}_{0.023}$  identifies four below-bandgap PL features and reveals anomalous negative thermal quenching at temperatures above 180 K. The low-energy A- and B-features manifest significant negative thermal quenching, while the high-energy C- and D-features quench monotonically, as temperature rises up. A phenomenological model is established for the negative thermal quenching mechanism that the residual electrons in the final state of the PL transition transfer into nonradiative states via thermal hopping, leading to increase in hole concentration and hence enhancement in PL recombination, and the activation energies of the

negative thermal quenching are deduced. The result indicates that the below-bandgap PL features are governed by carrier thermal hopping and nonradiative recombination in InPBi.

The authors thank Dr. Kai Wang for the samples. This work was supported by the MOST 973 Program (2014CB643901 and 2013CB632805), the NSFC (61604157 and 11274329) and the STCSM (16ZR1441400 and 16JC1402400) of China.

- <sup>1</sup>A. Kanjilal, L. Rebohle, S. Prucnal, M. Voelskow, W. Skorupa, and M. Helm, *Phys. Rev. B* **80**, 241313 (2009).
- <sup>2</sup>M. Trunk, V. Venkatachalapathy, A. Galeckas, and A. Y. Kuznetsov, *Appl. Phys. Lett.* **97**, 211901 (2010).
- <sup>3</sup>G. Callsen, M. R. Wagner, T. Kure, J. S. Reparaz, M. Bügler, J. Brunmeier, C. Nenstiel, A. Hoffmann, M. Hoffmann, J. Tweedie, Z. Bryan, S. Aygun, R. Kirste, R. Collazo, and Z. Sitar, *Phys. Rev. B* **86**, 075207 (2012).
- <sup>4</sup>H. Klasens, *Nature* **158**, 306 (1946).
- <sup>5</sup>M. A. Reshchikov, A. A. Kvasov, M. F. Bishop, T. McMullen, A. Usikov, V. Soukhoveev, and V. A. Dmitriev, *Phys. Rev. B* **84**, 075212 (2011).
- <sup>6</sup>T. Fuyuki, R. Yoshioka, K. Yoshida, and M. Yoshimoto, *Appl. Phys. Lett.* **103**, 202105 (2013).
- <sup>7</sup>R. B. Lewis, D. A. Beaton, X. Lu, and T. Tiedje, *J. Cryst. Growth* **311**, 1872 (2009).
- <sup>8</sup>J. Lee, J. Kim, and M. Razeghi, *Appl. Phys. Lett.* **70**, 3266 (1997).
- <sup>9</sup>B. Fluegel, S. Francoeur, A. Mascarenhas, S. Tixier, E. Young, and T. Tiedje, *Phys. Rev. Lett.* **97**, 67205 (2006).
- <sup>10</sup>X. Lu, D. Beaton, R. Lewis, T. Tiedje, and Y. Zhang, *Appl. Phys. Lett.* **95**, 041903 (2009).
- <sup>11</sup>S. Francoeur, M. Seong, A. Mascarenhas, S. Tixier, M. Adamczyk, and T. Tiedje, *Appl. Phys. Lett.* **82**, 3874 (2003).
- <sup>12</sup>S. Imhof, A. Thranhardt, A. Chernikov, M. Koch, N. Koster, K. Kolata, S. Chatterjee, S. Koch, X. Lu, S. Johnson, D. Beaton, T. Tiedje, and O. Rubel, *Appl. Phys. Lett.* **96**, 131115 (2010).
- <sup>13</sup>W. Pan, L. Zhang, L. Zhu, Y. Li, X. Chen, X. Wu, F. Zhang, J. Shao, and S. Wang, *J. Appl. Phys.* **120**, 105702 (2016).
- <sup>14</sup>M. K. Shakfa, M. Wiemer, P. Ludewig, K. Jandieri, K. Volz, W. Stolz, S. D. Baranovskii, and M. Koch, *J. Appl. Phys.* **117**, 025709 (2015).
- <sup>15</sup>K. Wang, Y. Gu, H. F. Zhou, L. Y. Zhang, C. Z. Kang, M. J. Wu, W. W. Pan, P. F. Lu, Q. Gong, and S. M. Wang, *Sci. Rep.* **4**, 5449 (2014).
- <sup>16</sup>Y. Gu, K. Wang, H. Zhou, Y. Li, C. Cao, L. Zhang, Y. Zhang, Q. Gong, and S. Wang, *Nanoscale Res. Lett.* **9**, 24 (2014).
- <sup>17</sup>X. Wu, X. Chen, W. Pan, P. Wang, L. Zhang, Y. Li, H. Wang, K. Wang, J. Shao, and S. Wang, *Sci. Rep.* **6**, 27867 (2016).
- <sup>18</sup>J. Kopaczek, R. Kudrawiec, M. P. Polak, P. Scharoch, M. Birkett, T. D. Veal, K. Wang, Y. Gu, Q. Gong, and S. Wang, *Appl. Phys. Lett.* **105**, 222104 (2014).
- <sup>19</sup>T. D. Das, *J. Appl. Phys.* **115**, 173107 (2014).
- <sup>20</sup>J. Shao, W. Lu, X. Lü, F. Yue, Z. Li, S. Guo, and J. Chu, *Rev. Sci. Instrum.* **77**, 063104 (2006).
- <sup>21</sup>J. Shao, Z. Qi, H. Zhao, L. Zhu, Y. Song, X. Chen, F.-X. Zha, S. Guo, and S. Wang, *J. Appl. Phys.* **118**, 165305 (2015).
- <sup>22</sup>P. Leyral, G. Bremond, A. Noukailhat, and G. Guillot, *J. Lumin.* **24–25**, 245 (1981).
- <sup>23</sup>H. Shibata, *Jpn. J. Appl. Phys.* **37**, 550 (1998).
- <sup>24</sup>X. Chen, Y. Song, L. Zhu, S. Wang, W. Lu, S. Guo, and J. Shao, *J. Appl. Phys.* **113**, 153505 (2013).
- <sup>25</sup>D. Kaplan, K. Mills, J. Lee, S. Torrel, and V. Swaminathan, *J. Appl. Phys.* **119**, 214301 (2016).
- <sup>26</sup>A. M. Stoneham, *Rev. Mod. Phys.* **41**, 82 (1969).
- <sup>27</sup>X. Zhang, J. Shao, L. Chen, X. Lü, S. Guo, L. He, and J. Chu, *J. Appl. Phys.* **110**, 043503 (2011).
- <sup>28</sup>X. Chen, J. Jung, Z. Qi, L. Zhu, S. Park, L. Zhu, E. Yoon, and J. Shao, *Opt. Lett.* **40**, 5295 (2015).
- <sup>29</sup>P. M. Mooney, K. P. Watkins, Z. Jiang, A. F. Basile, R. B. Lewis, V. Bahramiyekta, M. Masnadishirazi, D. A. Beaton, and T. Tiedje, *J. Appl. Phys.* **113**, 133708 (2013).
- <sup>30</sup>R. Kini, A. Ptak, B. Fluegel, R. France, R. Reedy, and A. Mascarenhas, *Phys. Rev. B* **83**, 075307 (2011).
- <sup>31</sup>P. Dreszer, W. M. Chen, K. Seendripu, J. A. Wolk, W. Walukiewicz, B. W. Liang, C. W. Tu, and E. R. Weber, *Phys. Rev. B* **47**, 4111 (1993).
- <sup>32</sup>W. Pan, P. Wang, X. Wu, K. Wang, J. Cui, L. Yue, L. Zhang, Q. Gong, and S. Wang, *J. Alloys Compd.* **656**, 777 (2016).
- <sup>33</sup>L. Wu, P. Lu, C. Yang, D. Liang, C. Zhang, and S. Wang, *J. Alloys Compd.* **674**, 21 (2016).